

Assessment of the efficiency and performance of different PV system configurations under various fault conditions

Raghad Adeeb Othman, Omar Sharaf Al-Deen Al-Yozbak

Department of Electrical Engineering, College of Engineering, University of Mosul, Mosul, Iraq

Article Info

Article history:

Received Mar 16, 2025

Revised Sep 3, 2025

Accepted Oct 2, 2025

Keywords:

Fault diagnosis

Ground fault

Power voltage curve

PV configurations

PV panels fault analysis

ABSTRACT

Partial shadowing, bypass-diode issues, photovoltaic (PV) module deterioration, and wiring issues are examples of PV failures that have a substantial effect on power production and cause distinct peaks in a PV system's P-V curves. Various PV fault types have been used in the solar cell system in this work. Four types were used: open circuit, line to ground, cross-line to line, and intra-line to line. The impact of various PV system failure types on the system's performance was emphasized in this study. MATLAB is used to display the simulation results for the four approaches (series parallel (SP), total cross tied (TCT), honeycomb (HC), and bridge link (BL)) under various fault scenarios. The current-voltage (I-V) and power-voltage (P-V) curves are used to compare the results for each fault scenario. The open circuit fault between PV (7.8) in the first string and PV (18.19) in the fourth string resulted in a 40% decrease in the short-circuit current of the photovoltaic system compared to its normal value in the SP topology, while in the HC and BL topologies, the current value exceeded the allowable limit. This, in turn, had an impact on the (I-V) characteristics of this topology. The fault's impact was minimal and within the typical bounds of its (I-V) characteristics in the TCT topology.

This is an open access article under the [CC BY-SA](#) license.



Corresponding Author:

Omar Sharaf Al-Deen Yehya Al-Yozbak

Department of Electrical Engineering, College of Engineering, University of Mosul

Mosul, Iraq

Email: o.yehya@uomosul.edu.iq

1. INTRODUCTION

The global renewable energy market has seen tremendous technological advancements due to the negative climate implications of fossil fuel-based power facilities. The increased governmental incentives and ongoing technology advancements aimed at lowering carbon footprints have made distributed generation (DG) using renewable resources increasingly appealing [1], [2]. The worldwide energy demand per person is rising as a result of the acceleration of industrial expansion and the ongoing rise in energy consumption. This cleared the path for in-depth study of novel green power technologies, including geothermal, biomass, hydro, wind, and solar power. These technologies are safe and sustainable.

Research on renewable energy technology is primarily concerned with converting renewable resources into electrical energy to support consumer loads or the utility grid [3]. Over the past few years, the solar company has grown quickly, with photovoltaic (PV) systems seeing the most expansion. One of the most important ways to improve the PV system's lifespan, dependability, and efficiency is to identify and anticipate different defects [4], [5]. PV malfunctions, including partial shadowing, bypass-diode malfunctions, PV module degradation, and wiring problems, significantly impact power output and result in different peaks in a PV system's P-V curves [6], [7]. A few things need to be made sure of in order to maximize the amount of energy harvested by photovoltaic systems: optimal irradiance levels, low

temperatures for PV cells, proper positioning and orientation of the panels toward the sun, and avoiding areas of shade. The dependability and efficiency of the entire PV installation are lowered by dirt, snow, and sand, which obscure solar irradiation. For this reason, the connections between PV modules and the cleanliness of PV panels play a critical role in the production of energy. Regular maintenance and diagnosis are increasingly important for this reason. The relevance of PV systems has increased due to the solar industry's tremendous rise in recent years. To improve solar PV array dependability, efficiency, and safety, fault analysis is essential. If faults go undetected, power generation may be reduced, system aging may speed up, and the availability of the entire system may be in jeopardy [8].

Global installations of large-scale solar PV power plants have grown impressively quickly in the last several years. Since the majority of these systems have multi-MW ratings and capabilities, they are made up of thousands of modules dispersed over hectares of land [9]. Keeping an eye on all these elements separately is time-consuming, expensive, and frequently not feasible. According to investigations, a number of factors, including extended outdoor operation, poor maintenance, enclosure issues, thermal cycling, grounding issues, and corrosive conditions, can cause PV modules to deteriorate prematurely [10]. The advantages of free solar energy for the environment and economy have made the PV sector more well-known in recent years. The total installed PV capacity is anticipated to increase to 438 GW between 2017 and 2022 [11]. Photovoltaic (PV) array fault analysis is thought to be crucial for raising the system's efficiency and safety. In addition to decreasing efficiency, faults shorten a system's lifespan [12]. PV panels are becoming more and more common. Their flaws, risks, and hazards are increasingly being used as a focal point for research to lower associated risks and accidents [13].

Despite the steady increase in the world's PV capacity, defect detection in PV systems is still a need that has not received enough attention [14]. Because of its many safety features, NEC article 690 is extensively used worldwide in the context of line-line (LL) and line-ground (LG) fault detection in PV arrays. Sadly, reports in the literature also indicate that NEC 690 standards have limits when it comes to identifying LL and LG errors [15]–[17]. Defect identification in solar PV arrays is an essential duty to boost PV systems' dependability, effectiveness, and security. Uncleaned faults in PV arrays not only result in power losses but also have the potential to generate safety concerns and fire threats if improper fault detection is carried out [18]. Regrettably, compared to the lightning-fast progress made in the field of maximum power point tracking thus far, awareness of PV defect detection is comparatively quite slow, maximum power point tracking (MPPT) [19]. Modern research on fault diagnosis in PV arrays is driven by the increasing prevalence of PV systems in modern electricity grids [20]. Electrical faults in PV arrays, especially LG and LL faults, pose a significant obstacle to the rapid advancement of PV power generation worldwide. Therefore, given the numerous unique operating characteristics of PV-producing systems, a thorough study of the compatibility of the LL/LG fault prevention standards specified for PV arrays is necessary [21].

Ground faults have the potential to go unnoticed and result in significant harm to both the PV array and the surrounding environment because of certain limitations in traditional detection procedures. Similar circumstances could occur in the event of line-to-line errors [22]. When any DC carrying conductor in one of these systems unintentionally connects to the earth or a grounded surface, a ground fault occurs. When ground faults arise, dc leakage becomes more intense and travels across the earth or other conductive pathways before coming back to the source [17]. PV installations comply with standards such as IEEE Standard 1374, National Electric Code (NEC) 690, and European International Electro Technical Commission Standard (IEC) 62548. LL and LG fault detection features have also been included to power conversion equipment (PCE) safety standards such as IEC 62109-1, IEC 62109-2, and Underwriters Laboratories UL 1741 in recent years. Thus, a thorough analysis of these standards' ability to identify LL and LG errors is also necessary. While there are many PV array problems, some have received more attention than others, including line-to-line faults (LLF), ground faults (GF), arc faults (AF), and hot spot faults (HSF) [23].

In this paper, different types of PV faults have been applied to a solar cell system. Four types, such as intra-line to line, cross-line to line, line to ground, and open circuit fault, these faults were applied in this work. This proposed PV system consists of a 5×5 matrix of PV arrays. The simulation results of the four methodologies (SP – TCT – HC – BL) under various fault cases are presented in MATLAB. The obtained results are compared in terms of the (I-V) curve and P-V curve all fault scenarios. In standard test condition (STC) (irradiance 1000 W/m², cell temperature 25 °C) the four topologies give the same (I-V) and (P-V) characteristics.

2. METHOD AND TOOLS

Single PV cell can produce tiny generated power and for high power proposes or grid connections, a group of parallel and series arrangements of PV cells to produce the required power for such applications. These kinds of arrangements are called PV modules which they form the PV panels. In this work a PV panel

with specification listed in Table 1 has been used as shown in Figure 1. A collection of linked solar modules, each with many solar panels, is called a solar array. Photovoltaic arrays, another name for solar arrays, are erected to supply enormous amounts of energy to residential and commercial structures.

In this work, MATLAB/Simulink was used to model a 5×5 PV array for various PV array topologies, where each module consists of 36 cells connected in series. A bypass diode is linked to every module. By controlling the output value of the voltage source (112 V) to linearly increase, the output current and voltage of the PV string are recorded, the associated data is then entered into the MATLAB workspace to produce the (I-V) characteristic curve. A blocking diode is used in the PV string's output to prevent negative currents from occurring. As illustrated in Figure 2, the impact of the most frequent flaws in the PV array characteristics on the array's performance was studied at STC in constant weather circumstances.

Table 1. PV module specifications

| (PV module) parameter | Value |
|--|------------|
| Maximum power (P _{MAX}) | 170 W |
| Voltage at maximum power (V _{mp}) | 18.3 V |
| Current at maximum power (I _{mp}) | 9.29 A |
| Open circuit voltage (V _{oc}) | 22.4 V |
| Short circuit current (I _{sc}) | 10.22 A |
| Temperature coefficient of V _{oc} (K _v) | -0.29 V/°C |
| Temperature coefficient of I _{sc} (K _i) | -0.05 A/°C |
| Maximum power (P _{MAX}) | 170 W |



Figure 1. PV panel and name plate specification

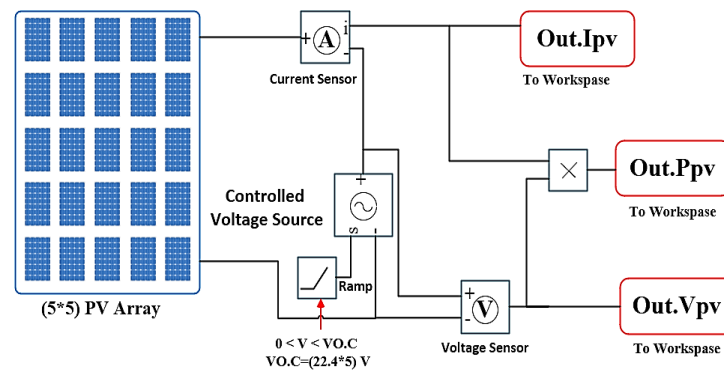


Figure 2. (I-V) & (P-V) testing circuit of PV array modelling via MATLAB/Simulink

3. PV ARRAY TOPOLOGIES

The topology of series and parallel PV panels has some drawbacks, such as less current and voltage. Therefore, many configurations of PV arrays have been proposed in this field that which is commonly categorized as [24]:

3.1. Series-parallel (SP)

Although a series-parallel PV model connection cannot improve voltage and current range at the same time, it is still preferred because of its low cost, minimal electrical losses, good dependability, and it

differs from the series topology in that it has fewer mismatch losses. Because it has fewer series modules than the total number of series modules connected in a topological series. As seen in Figure 3, an arrangement of five modules connected in series complying strings five of these strings joined in parallel to obtain the SP configuration. The most popular configuration, series-parallel, is simple to utilize. Although the series and parallel configurations increase the PV system's overall output, they have the disadvantage of being less effective when there is partial shading.

3.2. Total cross tied (TCT)

Unlike SP, the TCT configuration is retrieved from the topology of SP, although it is more difficult to implement. As seen in Figure 4, it features a cross-rows and cross-columns connected arrangement where the total voltage and total current are equal throughout all rows and all columns, respectively. The TCT scheme has the drawback of having more times than SP, which raises cable losses even though it performs better than SP in terms of shading and mismatch losses.

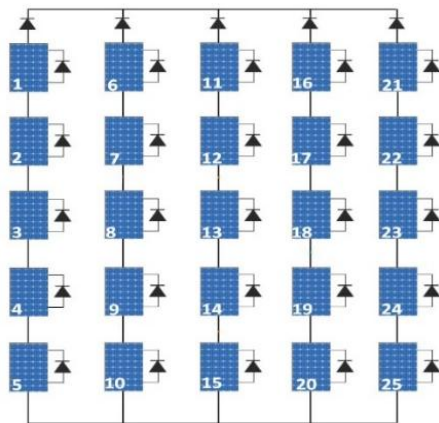


Figure 3. SP topologies of (5×5) PV array

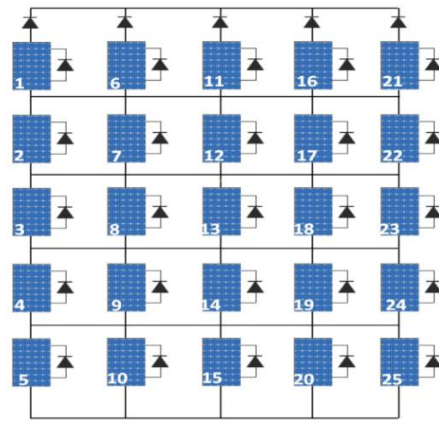


Figure 4. TCT topologies of (5×5) PV array

3.3. Bridge linked (BL)

The bridge-linked topology, as illustrated in Figure 5, is derived from TCT and has the advantages of requiring fewer connections, requiring less time to build the wiring, and having fewer cable losses; however, under shading conditions, it has a negative impact on the total voltage and current.

3.4. Honeycomb (HC)

This topology is based on the TCT concept, which uses a honeycomb structure. As seen in Figure 6, the connection shape of the ties differs slightly from BL. Although output power losses in this design can be lowered, it is limited in that power losses cannot be reduced in all shading conditions.

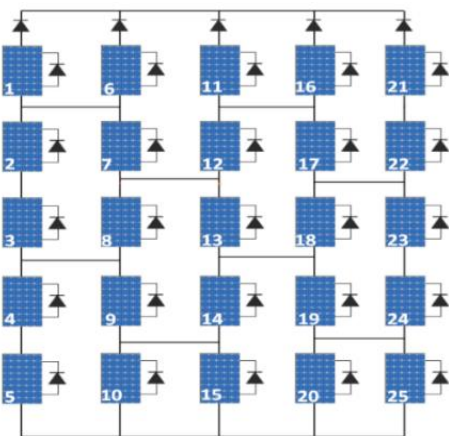


Figure 5. BL Topologies of (5×5) PV array

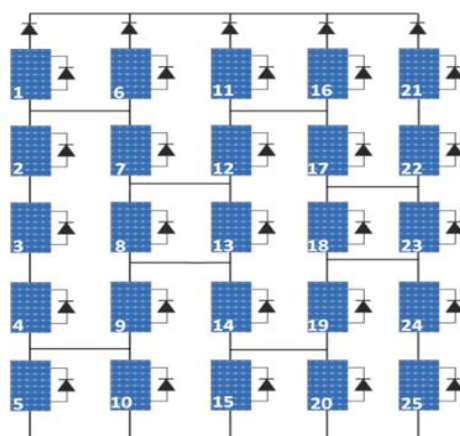


Figure 6. HC Topologies of (5×5) PV array

4. FAULTS IN PV ARRAYS

Two typical fault scenarios for PV arrays exist [25]. Electrical issues are the first, while shade faults are the second. Anomalies that arise in the system's internal electrical architecture are the cause of electrical problems. However, changes in the external environment and isolation levels are causing shade defects [26]. As shown in Figure 7, the three most prevalent types of electrical faults are i) line to line (L-L), ii) line to ground (L-G), and iii) open circuit (OC). These issues could lead to decreased power production and possibly irreversible harm to the photovoltaic system [17]. When there is a short circuit between any two locations in the PV array, line-to-line faults are produced. Furthermore, interesting and cross-string faults are LL faults that occur in both the same string and two distinct strings. Significant problems, such as power outages, possible damage to the PV modules, and safety risks, can result from this kind of malfunction. Low irradiance makes it challenging to identify LL faults with low levels of mismatch fault because the fault current is of a small size and goes unnoticed. The number of PV modules involved in the fault is indicated by this mismatch level. The mismatch level and fault path impedance are the two main factors that determine how severe an LL fault is. The fault current will be minimal if the mismatch level is low and the impedance is high [27].

The connection between the earth ground conductor (EGC) and the current-carrying conductor (CCC) is the usual cause of LG faults, although they can also originate from internal PV cell failure or cable insulation failure. An LG fault occurs due to a blocking diode and zero fault resistance. Modules are identified by their location in the PV array. The current from the defective modules might even go in two different directions: either via the short-circuit route or through the healthy module. An open circuit defect is any situation in when there is an open circuit between two panels that prevents power from flowing. Many factors can cause overcurrent faults (OC faults), including a broken cable between two strings, an object falling on the panels, a bad connection between two locations, or an unintentional break in a current-carrying conductor [12]. Arc faults, on the other hand, result from open circuit faults in a string or from insulation failure between two portions of adjacent strings. They can occur in parallel or sequence and pose a serious risk for fire.

In this work, four PV system topologies are connected to be investigated under four common electrical faults, as shown in Figure 7. Such as: i) cross string line-line fault, ii) intra string line-line fault, iii) line to ground fault, and iv) open circuit fault. These kinds of faults are considered the most common of electrical faults, with an incidence percentage of about 30% to 60% of all faults, depending on the PV cell circumstances regarding to the installation and the environment [28]. Each of the chosen topologies consists of a PV array (5×5) built in MATLAB/Simulink with solar modules having the data as listed in Table 1 under STC.

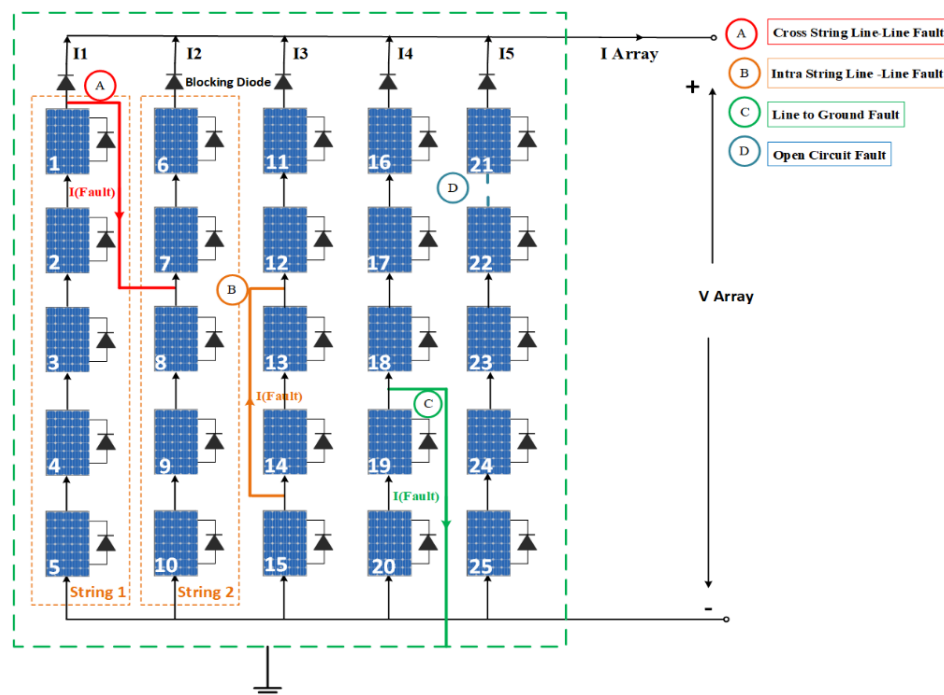


Figure 7. PV system under four electrical faults

5. RESULTS AND DISCUSSION

This section presents the MATLAB simulation results for the four techniques (SP, TCT, HC, and BL) under different fault scenarios. For every failure scenario, the resulting results are compared using the (I-V) and (P-V) curves. As indicated in Table 2, under typical circumstances, all four topologies at STC provide the same (I-V) & (P-V) properties. When operating faultlessly in all four topologies, the PV array's generating output power is 4.2163 K watts (STC) at 1000 W/m² of irradiance and 25 °C in temperature.

Table 2. PV array output at STC

| Topology | Vo.c (V) | Is.c (A) | Vmax (V) | Imax (A) | PMPP (W) |
|----------|----------|----------|----------|----------|----------|
| SP | 111.3 | 51.73 | 91.16 | 46.28 | 4216.3 |
| TCT | 111.4 | 51.73 | 91.01 | 46.26 | 4216.27 |
| HC | 111.4 | 51.73 | 91.10 | 46.24 | 4216.3 |
| BL | 111.4 | 51.73 | 91.10 | 46.24 | 4216.3 |

5.1. Cross string line–line fault in the PV array

There's a problem between these two strings. Figure 8 results demonstrate that, for the (P-V) characteristics, the whole range of the (I-V) characteristics remains unaffected in the SP topology, irrespective of the number of panels impacted by the fault. The maximum power reached 3680.66 watts when the fault between PV1 and PV7 occurred because the voltage value in the SP topology was 12.3% lower than it was in the typical scenario. Since it is the current from the non-faulty strings that can go straight into the faulty string in the event of a short circuit, avoiding the load. This may result in overcurrent in the impacted strings, harming these modules. Similar to the SP topology, the defect causes current from non-faulty strings to be diverted into the faulty strings, but the cross-ties allow for some current redistribution across the PV array. Depending on the number of panels implicated in the failure, it is discovered that the open circuit voltage in the TCT topology decreases dramatically. Since the defect was between PV1 and PV10, the voltage dropped by 60.3%, which had a significant impact on the system's functionality. The TCT topology saw a reduction in the majority of the power generated at this fault. If the maximum power value drops to 1410.95 watts when the fault happens between PV1 and PV10. Though, depending on how the problem affects the system, some power might still be available from unaffected strings.

Because there is less chance of an excessive current in any one string due to the more even distribution of current throughout the array, the HC topology provides superior protection for the modules. In comparison to SP and TCT topologies, the power loss is less severe, although the array output will still be impacted. If the fault arises between PV1 and PV10, the maximum power in HC drops to 1694.83 watts. Depending on how serious and where the defect is, the system can still function less efficiently. In BL topology, the bridge connections facilitate alternating current routes in the event of a cross-string line-line fault. This effectively isolates the fault and reduces its influence on the remaining portions of the array. The impact of a defect occurring in both the HC and BL topologies is comparable. When the number of panels impacted by the problem rises, it is evident how the fault reduces the open circuit voltage; nevertheless, this effect is not as great as it would be in a TCT architecture.

5.2. Intra string line–line fault in the PV array

A direct short circuit between two places in the same string is caused by the defect. Table 3 shows the results of highlighting the error in each of the four topologies. This reduces the number of active modules in the string by creating a bypass for the current in the SP topology around the section of the string between the fault spots. As a result, the damaged string's voltage output dramatically decreases. Because the voltage of the afflicted string is lower, the PV array's overall power output is decreased. Nevertheless, depending on how serious the error is, some strings might keep working as they should. It is observed that the short-circuit current was not impacted by the fault, irrespective of the number of panels impacted, and consequently, the overall range (I-V) characteristics in the SP architecture were not impacted. allows the current to be redistributed throughout the PV array in the TCT design, potentially lessening the effect on the system as a whole. The impacted string's voltage output decreases, but because the cross-ties enable other strings to make up for the loss, the voltage across the array is stabilized. A significant drop in the open circuit voltage is observed to change the (I-V) characteristics of the TCT topology, depending on how many panels are affected by the fault. Furthermore, the maximum voltages dropped as the number of defective panels in a string rose, affecting the (P-V) characteristics of this system. As a result, when the malfunction happened at PV, less electricity was generated at 1410.45 watts (1,2,3,4). Three sequential PV models (1, 2, and 3) within one string in the HC and BL topologies experienced significant wave distortion [18] and open circuit voltage readings outside of the permitted range.

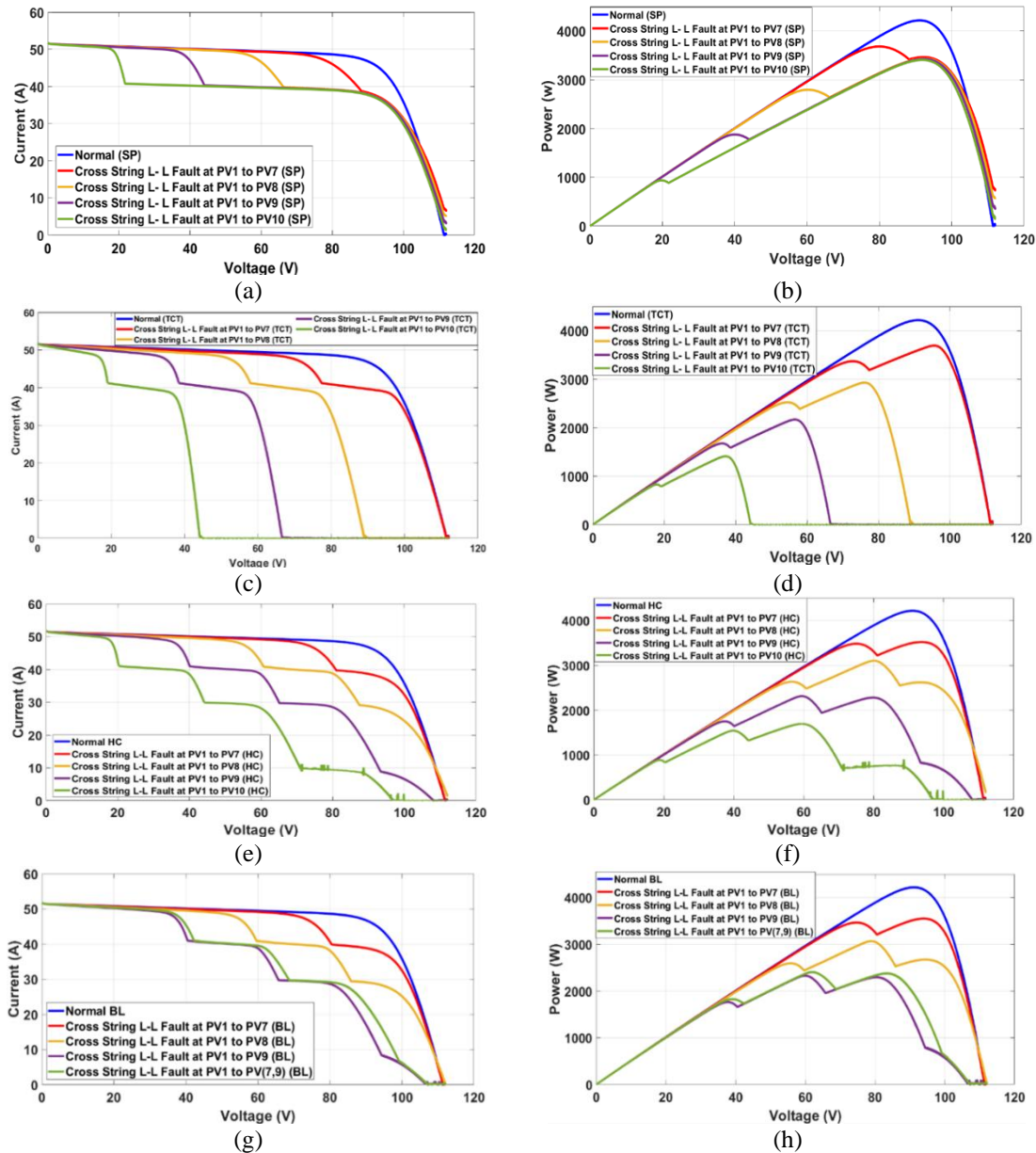


Figure 8. PV array characteristics under cross line – line fault: (a) (I-V) curve for SP; (b) (P-V) curve for SP; (c) (I-V) curve for TCT; (d) (P-V) curve for TCT; (e) (I-V) curve for HC; (f) (P-V) curve for HC; (g) (I-V) curve for BL; and (h) (P-V) curve for BL

Table 3. PV array performance under intra line – line fault

| Fault location | Topology | Vo.c (V) | Is.c (A) | Vmax (V) | Imax (A) | Pmpp (W) |
|-----------------|----------|----------|----------|----------|----------|----------|
| At PV1 | SP | 111.4 | 51.73 | 79.95 | 46 | 3680.63 |
| | TCT | 111.4 | 51.73 | 95.55 | 38.65 | 3692.38 |
| | HC | 111.4 | 51.73 | 93.66 | 37.6 | 3519.78 |
| | BL | 111.4 | 51.73 | 93.89 | 37.8 | 3549.47 |
| At PV(1,2) | SP | 111.4 | 51.73 | 91.00 | 37 | 3376.26 |
| | TCT | 89 | 51.73 | 76.07 | 38.5 | 2982.87 |
| | HC | 110.86 | 51.73 | 83.75 | 38.33 | 3210.43 |
| | BL | 110.86 | 51.73 | 82.02 | 38.41 | 3153.32 |
| At PV (1,2,3) | SP | 111.4 | 51.73 | 91.10 | 37 | 3373.03 |
| | TCT | 66.96 | 51.73 | 56.6 | 38.27 | 2167.84 |
| | SP | 111.4 | 51.73 | 90.86 | 37 | 3377.03 |
| At PV (1,2,3,4) | TCT | 44.4 | 51.73 | 37 | 38.11 | 1410.45 |
| | HC | 97.7 | 51.73 | 59.99 | 28.6 | 1716.72 |
| At PV (1, 3, 4) | BL | 105.5 | 51.73 | 63.78 | 38.38 | 2448.15 |

5.3. Line – ground fault in the PV array

Table 4 illustrates that the (I-V) features of the SP topology were unaffected by this fault, regardless of its location, when it was projected between the string and ground cells. When a line-ground fault happens in the SP topology, the impacted string or module may provide a low-resistance channel to the ground. The current flow through the ground path may significantly rise as a result of this. A voltage imbalance in the impacted string due to the defect may result in a decrease in the string's overall output voltage. Due to the loss of the string current that caused the fault, we observe a decrease in the maximum current value to 37 A. In contrast, the open circuit voltage remained at its normal value, with the exception of the last case, in which PV5 was impacted by the fault, and the maximum voltage value was noted to have decreased by 12% from its value in the normal case. The failure at PV3 to ground would cause the maximum power output to drop to 3375.23 watts. When using TCT topology, the defect may cause the voltage in the impacted string to drop, much like in the SP topology. Because the strings are interconnected, the TCT topology may be able to partially alleviate this voltage drop, but the overall output of the array will still be impacted.

The location of the fault and the efficiency of the cross-ties in redistributing the current determine how much of a reduction in power output occurs. It's possible that the array will keep running less efficiently. The findings suggest that when the fault was concentrated at the start of the string and the ground, the TCT topology saw the largest fall in the values of the open circuit voltage and short circuit current. This, in turn, had an impact on the (I-V) characteristics of this topology. The voltage drop was near when the fault happened between PV1 and ground or PV2 and earth, but the largest current value occurred when the failure happened between PV1 and ground because the string current leaked to ground. The other problem locations did not experience any change in the maximum current value.

5.4. Open-circuit fault in the PV array

Testing an open circuit fault within one of the strings reveals that, as seen in Figure 9, it is clear how faults affect current reduction in SP topology. Due to the string current loss where the fault occurs, this effect manifests when the fault happens in any string inside this topology. The damaged string doesn't provide any power; hence, the overall output of the array is decreased even though the other parallel strings are running normally. The amount of impacted strings directly correlates with the power loss.

This is demonstrated by the fact that when a fault occurs in one string, the maximum power value lowers from its normal value of 4216.3 watts to 3373.01 watts, and when a fault occurs in two strings, the power drops to 2529.78 watts. The current from the other parallel modules is redistributed through the other functional modules at the TCT topology when an open-circuit fault occurs in one of the modules. Although the array's output is decreased, it can still provide power. In comparison to the SP arrangement, the TCT configuration minimizes power loss by enabling surrounding strings to adjust for the voltage of the malfunctioning string. Consequently, we discover that the TCT topology experienced the least reduction in maximum power, dropping to 3692.31 watts. Better current redistribution is possible in the event of an open-circuit fault with the HC configuration. Since the problematic module's current is more efficiently distributed among nearby modules, the impact of the failure is reduced. The greatest power in this topology was 3413.75 watts. However, in BL Topology, the bridge connections permit the current to travel through the defective string in the event of an open-circuit malfunction. The array's output is barely changed, and the unaffected modules keep running. Because of the way the BL topology isolates the problematic module, there is less disturbance to the remainder of the array's functionality. The maximum power drops to 3449.14 according to the results.

Table 4. PV array performance under line-ground fault

| Fault location | Topology | Vo.c (V) | Is.c (A) | Vmax (V) | Imax (A) | Pmpp (W) |
|----------------|----------|----------|----------|----------|----------|----------|
| From PV1 | SP | 111.4 | 51.73 | 91.10 | 37 | 3373.03 |
| | TCT | 22.47 | 41.38 | 18.69 | 37 | 692.92 |
| | BL | 68.92 | 41.34 | 39.27 | 28.17 | 1105.24 |
| From PV2 | SP | 111.4 | 51.73 | 91.01 | 37 | 3368.78 |
| | TCT | 21.73 | 51.73 | 17.78 | 46.5 | 828.57 |
| | BL | 68.02 | 51.73 | 38.55 | 27.99 | 1083.97 |
| From PV3 | SP | 111.4 | 51.73 | 91.05 | 37 | 3373.03 |
| | TCT | 44.11 | 51.73 | 36.24 | 46 | 1675.64 |
| | BL | 90.41 | 51.73 | 39.03 | 46.85 | 1827.93 |
| From PV4 | SP | 111.4 | 51.73 | 91.20 | 37 | 3375.23 |
| | TCT | 66.5 | 51.73 | 54.40 | 46.2 | 2522.43 |
| From PV5 | SP | 111.4 | 51.73 | 79.95 | 38.9 | 3680.63 |
| | TCT | 88.9 | 51.73 | 72.8 | 46.33 | 3369.4 |
| | HC | 106.6 | 51.73 | 74.98 | 46.43 | 3481.53 |
| | BL | 105.54 | 51.73 | 76.49 | 46.34 | 3539.71 |

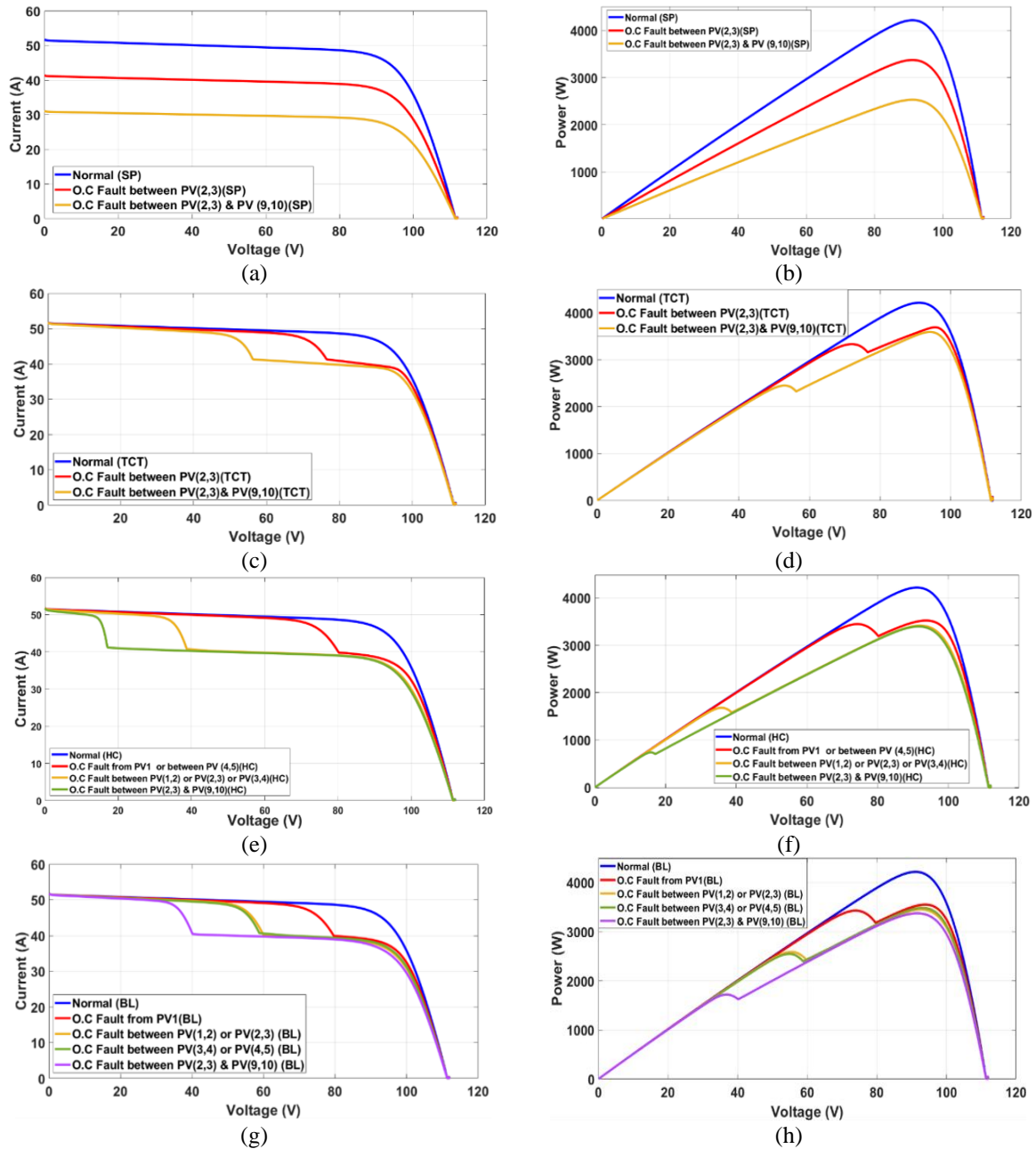


Figure 9. PV array characteristics under open circuit fault: (I-V) curve for SP; (b) (P-V) curve for SP; (c) (I-V) curve for TCT; (d) (P-V) curve for TCT; (e) (I-V) curve for HC; (f) (P-V) curve for HC; (g) (I-V) curve for BL; and (h) (P-V) curve for BL

5.5. Comparison of performance of the PV array configurations

In order to compare the performance of the four topologies when faults occurred, these faults were placed in the same location for all of these topologies at STC, and the results showed in Figure 10 that, the effect of the open circuit fault between PV (7,8) in the first string and PV (18,19) in the fourth string, it led to a decrease in the short-circuit current of the photovoltaic system by 40% from its value in the normal state in the SP topology, while the value of this current increased beyond the permissible limit in the HC and BL topologies, and this in turn affected the (I-V) characteristics of this topology. While in the TCT topology, the effect of the fault was limited and within the normal limits of its (I-V) characteristics.

As for the (P-V) characteristics, the performance of the TCT was better than the other topology, as it had the highest power generated under the influence of this fault. As for the SP, the power generated under the influence of this fault decreased significantly, reaching 40% of its value in the normal state. When the

intra-line-line fault was imposed between PV (1,2) in the four topologies, it led to a decrease in the value of the open circuit voltage by 40.3% from its value in the normal case in the TCT topology. There was a significant distortion [29] in the characteristics of the HC topology, despite the closeness of the results between it and the BL topology. The (P-V) characteristics under the influence of this fault were the best in the SP topology, as it gave the highest generated power, as shown in Figure 11.

When the cross-line – line fault is highlighted between PV1 in the first string and PV8 in the second string, we notice the effect of the fault in decreasing the open circuit voltage in the TCT topology, which affected its (I-V) characteristics as shown in Figure 12. This fault also affected the (P-V) characteristics of this topology. The (I-V) and (P-V) characteristics of the HC and BL topologies are very similar. Despite the occurrence of distortion, the dynamic and intricate interactions that occur within the photovoltaic array as it attempts to redistribute current, regulate voltage, and preserve overall system balance are the main cause of the noise shown in the P-V curve. The P-V curve exhibits abnormalities or noise due to transient effects, voltage variations, and harmonic distortions caused by these interactions. Although the BL & HC architecture is intended to reduce the impact of failures, the quick modifications and adjustments necessary to isolate the fault and redistribute power may cause momentary disruptions in the output characteristics of the system, the HC wave [29]–[31]. The SP & BL topology had the best performance under the influence of this fault.

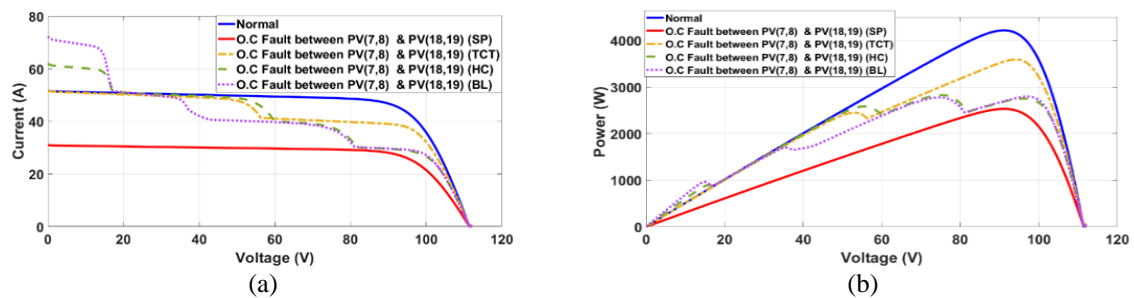


Figure 10. PV array characteristics under open circuit fault: (a) (I-V) curve and (b) (P-V) curve

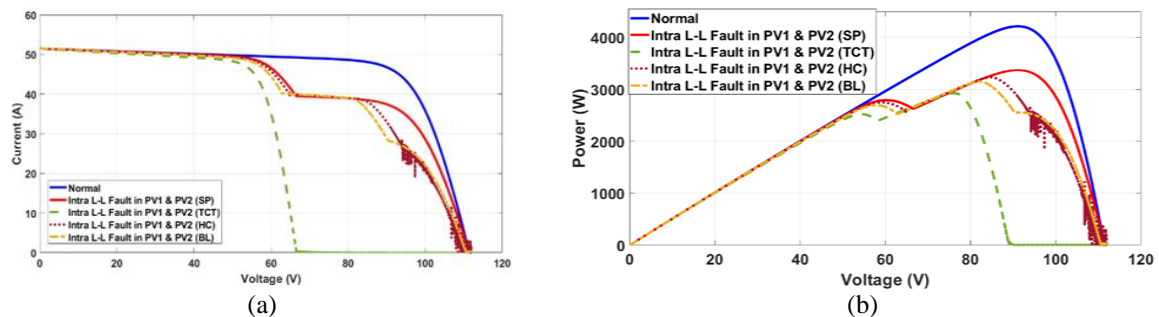


Figure 11. PV array characteristics under intra line – line fault: (a) (I-V) curve and (b) (P-V) curve

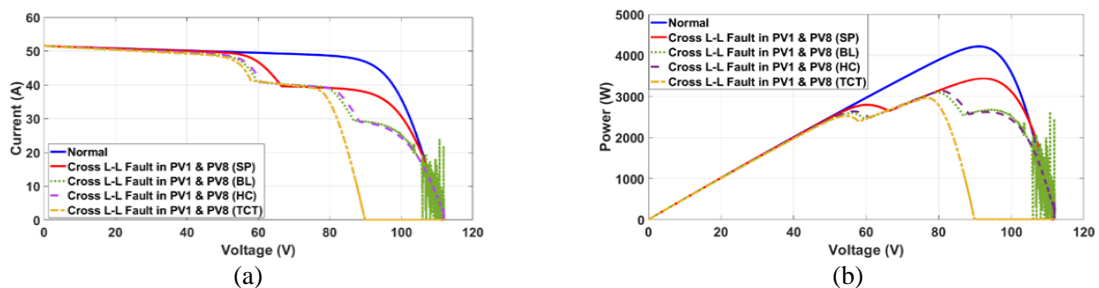


Figure 12. PV array characteristics under cross line – line fault: (a) (I-V) curve and (b) (P-V) curve

Line-to-line faults in electrical networks can be closely associated with the PV system's power curve spikes. A sudden short-circuit condition between two phases results in a rapid rise in current during a line-to-line fault. This causes a brief disruption in the system, which causes a sudden increase in power when the

fault briefly produces a high-power state. Before preventive devices like relays or circuit breakers turn on to isolate the fault, these spikes show how the system responded to the fault right away. Identification and mitigation of such incidents can be facilitated by analyzing these spikes, which can yield important insights on fault detection and system stability. As for the line – ground fault from PV15 in the third and ground string as shown in Figure 13, it led to a decrease in the open circuit voltage in the TCT, HC and BL topologies. Which affected their (I-V) characteristics. The (P-V) characteristics of the HC and BL topologies were very similar. The characteristics of the SP topology were the best in this case.

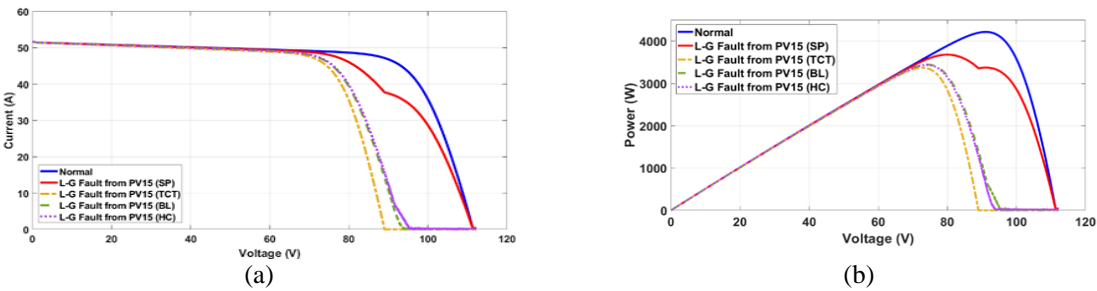


Figure 13. PV array characteristics under line – ground fault: (a) (I-V) curve and (b) (P-V) curve

6. CONCLUSION

This study emphasized the impact of various PV system failure types on the system's performance. In MATLAB, the simulation results for the four methodologies (SP, TCT, HC, and BL) under various failure scenarios are displayed. The obtained results are compared for each fault scenario using the I-V and P-V curves. When compared to other topologies at the same fault site, the open circuit failure was determined to have the least effect on the TCT topology because it generated the highest maximum power. The TCT topology offers a balanced solution with moderate fault tolerance and complexity. Regarding the effects of both intra- and cross-string line-line faults, the SP and BL topologies fared the best. The BL topology offers the best fault tolerance with the least amount of impact on performance and safety, making it perfect for large, crucial applications where reliability is crucial. It also significantly lowers the risk of module damage and allows the array to continue operating with minimal power loss because it can reroute current away from the fault. The choice of topology depends on the particular requirements of the PV system, such as its size, the significance of fault tolerance, cost considerations, and the necessity of sustaining continuous power output. Each topology offers varying degrees of fault tolerance and complexity.

ACKNOWLEDGMENTS

The authors would like to thank University of Mosul, College of Engineering, Electrical Department, for the support given during this work.

FUNDING INFORMATION

Authors state no funding involved.

AUTHOR CONTRIBUTIONS STATEMENT

This journal uses the Contributor Roles Taxonomy (CRediT) to recognize individual author contributions, reduce authorship disputes, and facilitate collaboration.

| Name of Author | C | M | So | Va | Fo | I | R | D | O | E | Vi | Su | P | Fu |
|---------------------|---|---|----|----|----|---|---|---|---|---|----|----|---|----|
| Raghad Adeeb Othman | ✓ | ✓ | ✓ | ✓ | ✓ | ✓ | ✓ | ✓ | ✓ | ✓ | ✓ | | | |
| Omar Sharaf Al-Deen | ✓ | ✓ | ✓ | ✓ | | ✓ | | ✓ | ✓ | ✓ | ✓ | ✓ | ✓ | |
| Yehya Al-Yozbaky | | | | | | | | | | | | | | |

| | | |
|-----------------------|--------------------------------|----------------------------|
| C : Conceptualization | I : Investigation | Vi : Visualization |
| M : Methodology | R : Resources | Su : Supervision |
| So : Software | D : Data Curation | P : Project administration |
| Va : Validation | O : Writing - Original Draft | Fu : Funding acquisition |
| Fo : Formal analysis | E : Writing - Review & Editing | |

CONFLICT OF INTEREST STATEMENT

Authors state no conflict of interest.

DATA AVAILABILITY

Data availability is not applicable to this paper as no new data were created or analyzed in this study.





REFERENCES

- [1] P. Verma, C. Singh, R. Dogra, M. S. Bhaskar, N. Gupta, and B. Khan, "Modeling and performance analysis of novel quad-tied PV array configuration under partial shading conditions," *Energy Science & Engineering*, vol. 11, no. 10, pp. 3434–3446, Oct. 2023, doi: 10.1002/ese3.1531.
- [2] R. A. Othman and O. S. A.-D. Al-Yozbaky, "Effect of reactive power capability of the PV inverter on the power system quality," *Indonesian Journal of Electrical Engineering and Informatics (IJEI)*, vol. 10, no. 4, pp. 780–795, Dec. 2022, doi: 10.52549/ijeiv10i4.3913.
- [3] S. R. Madeti and S. N. Singh, "A comprehensive study on different types of faults and detection techniques for solar photovoltaic system," *Solar Energy*, vol. 158, pp. 161–185, Dec. 2017, doi: 10.1016/j.solener.2017.08.069.
- [4] K. Abdulmawjood, S. S. Refaat, and W. G. Morsi, "Detection and prediction of faults in photovoltaic arrays: A review," *Proceedings - 2018 IEEE 12th International Conference on Compatibility, Power Electronics and Power Engineering, CPE-POWERENG 2018*, pp. 1–8, 2018, doi: 10.1109/CPE.2018.8372609.
- [5] International Renewable Energy Agency, "Renewable energy statistics 2021," 2021. [Online]. Available: www.irena.org
- [6] A. Ul-Haq, R. Alammari, A. Iqbal, M. Jalal, and S. Gul, "Computation of power extraction from photovoltaic arrays under various fault conditions," *IEEE Access*, vol. 8, pp. 47619–47639, 2020, doi: 10.1109/ACCESS.2020.2978621.
- [7] S. Kouro, J. I. Leon, D. Vinnikov, and L. G. Franquelo, "Grid-connected photovoltaic systems: an overview of recent research and emerging PV converter technology," *IEEE Industrial Electronics Magazine*, vol. 9, no. 1, pp. 47–61, Mar. 2015, doi: 10.1109/MIE.2014.2376976.
- [8] M. S. Arani and M. A. Hejazi, "The comprehensive study of electrical faults in PV arrays," *Journal of Electrical and Computer Engineering*, vol. 2016, no. 1, 2016, doi: 10.1155/2016/8712960.
- [9] R. A. Othman and O. S. A.-D. Y. Al-Yozbaky, "Influence of reactive power compensation from PV systems on electrical grid," *International Journal of Power Electronics and Drive Systems (IJPEDS)*, vol. 14, no. 2, pp. 1172–1183, Jun. 2023, doi: 10.11591/ijpeds.v14.i2.pp1172-1183.
- [10] J. P. Ram, H. Manghani, D. S. Pillai, T. S. Babu, M. Miyatake, and N. Rajasekar, "Analysis on solar PV emulators: A review," *Renewable and Sustainable Energy Reviews*, vol. 81, pp. 149–160, Jan. 2018, doi: 10.1016/j.rser.2017.07.039.
- [11] A. Khoshnami and I. Sadeghkhani, "Fault detection for PV systems using Teager-Kaiser energy operator," *Electronics Letters*, vol. 54, no. 23, pp. 1342–1344, 2018, doi: 10.1049/el.2018.6510.
- [12] S. Gul, A. U. Haq, M. Jalal, A. Anjum, and I. U. Khalil, "A unified approach for analysis of faults in different configurations of PV arrays and its impact on power grid," *Energies*, vol. 13, no. 1, p. 156, 2019, doi: 10.3390/en13010156.
- [13] B. Nehme, N. K. Msirdi, A. Namaane, and T. Akiki, "Analysis and characterization of faults in PV panels," *Energy Procedia*, vol. 111, pp. 1020–1029, Mar. 2017, doi: 10.1016/j.egypro.2017.03.265.
- [14] D. S. Pillai, F. Blaabjerg, and N. Rajasekar, "A comparative evaluation of advanced fault detection approaches for PV systems," *IEEE Journal of Photovoltaics*, vol. 9, no. 2, pp. 513–527, Mar. 2019, doi: 10.1109/JPHOTOV.2019.2892189.
- [15] D. S. Pillai and N. Rajasekar, "An MPPT-based sensorless line-line and line-ground fault detection technique for PV systems," *IEEE Transactions on Power Electronics*, vol. 34, no. 9, pp. 8646–8659, 2018, doi: 10.1109/TPEL.2018.2884292.
- [16] Y. Zhao, J. F. De Palma, J. Mosesian, R. Lyons, and B. Lehman, "Line-line fault analysis and protection challenges in solar photovoltaic arrays," *IEEE Transactions on Industrial Electronics*, vol. 60, no. 9, pp. 3784–3795, 2012, doi: 10.1109/TIE.2012.2205355.
- [17] M. K. Alam, F. Khan, J. Johnson, and J. Flicker, "A comprehensive review of catastrophic faults in PV arrays: types, detection, and mitigation techniques," *IEEE Journal of Photovoltaics*, vol. 5, no. 3, pp. 982–997, 2015.
- [18] Y. Zhao, L. Yang, B. Lehman, J. F. De Palma, J. Mosesian, and R. Lyons, "Decision tree-based fault detection and classification in solar photovoltaic arrays," *Conference Proceedings - IEEE Applied Power Electronics Conference and Exposition - APEC*, pp. 93–99, 2012, doi: 10.1109/APEC.2012.6165803.
- [19] M. Hlaili and H. Mechergui, "Comparison of different MPPT algorithms with a proposed one using a power estimator for grid connected PV systems," *International Journal of Photoenergy*, vol. 2016, pp. 1–10, 2016, doi: 10.1155/2016/1728398.
- [20] M. A. Sahnoun, H. M. R. Ugalde, J.-C. Carmona, and J. Gomand, "Maximum power point tracking using P&O control optimized by a neural network approach: a good compromise between accuracy and complexity," *Energy Procedia*, vol. 42, pp. 650–659, 2013, doi: 10.1016/j.egypro.2013.11.067.
- [21] M. M. Badr, M. S. Hamad, A. S. Abdel-Khalik, R. A. Hamdy, S. Ahmed, and E. Hamdan, "Fault identification of photovoltaic array based on machine learning classifiers," *IEEE Access*, vol. 9, pp. 159113–159132, 2021, doi: 10.1109/ACCESS.2021.3130889.
- [22] D. S. Pillai and R. Natarajan, "A compatibility analysis on NEC, IEC, and UL standards for protection against line-line and line-ground faults in PV arrays," *IEEE Journal of Photovoltaics*, vol. 9, no. 3, pp. 864–871, 2019.
- [23] M. A. Aftab, S. M. S. Hussain, I. Ali, and T. S. Ustun, "Dynamic protection of power systems with high penetration of renewables: A review of the traveling wave based fault location techniques," *International Journal of Electrical Power and Energy Systems*, vol. 114, p. 105410, 2020, doi: 10.1016/j.ijepes.2019.105410.
- [24] A. Y. Appiah, X. Zhang, B. B. K. Ayawli, and F. Kyeremeh, "Review and performance evaluation of photovoltaic array fault detection and diagnosis techniques," *International Journal of Photoenergy*, vol. 2019, Feb. 2019, doi: 10.1155/2019/6953530.
- [25] S. Sharma *et al.*, "Performance enhancement of PV system configurations under partial shading conditions using MS method," *IEEE Access*, vol. 9, pp. 56630–56644, 2021, doi: 10.1109/ACCESS.2021.3071340.
- [26] S. Voutsinas, D. Karolidis, I. Voyiatzis, and M. Samarakou, "Photovoltaic faults: a comparative overview of detection and identification methods," *2021 10th International Conference on Modern Circuits and Systems Technologies, MOCAST 2021*, no. 1–5, 2021, doi: 10.1109/MOCAST52088.2021.9493369.





- [27] F. Aziz, A. Ul Haq, S. Ahmad, Y. Mahmoud, M. Jalal, and U. Ali, "A novel convolutional neural network-based approach for fault classification in photovoltaic arrays," *IEEE Access*, vol. 8, pp. 41889–41904, 2020, doi: 10.1109/ACCESS.2020.2977116.
- [28] C. Yang *et al.*, "A survey of photovoltaic panel overlay and fault detection methods," *Energies*, vol. 17, no. 4, p. 837, 2024, doi: 10.3390/en17040837.
- [29] M. Bressan, Y. El Basri, A. G. Galeano, and C. Alonso, "A shadow fault detection method based on the standard error analysis of I-V curves," *Renewable Energy*, vol. 99, pp. 1181–1190, Dec. 2016, doi: 10.1016/j.renene.2016.08.028.
- [30] S. R. Pendem and S. Mikkili, "Modelling and performance assessment of PV array topologies under partial shading conditions to mitigate the mismatching power losses," *Solar Energy*, vol. 160, pp. 303–321, 2018, doi: 10.1016/j.solener.2017.12.010.
- [31] H. N. R. Suresh, S. Rajanna, S. B. Thanikanti, and H. H. Alhelou, "Hybrid interconnection schemes for output power enhancement of solar photovoltaic array under partial shading conditions," *IET Renewable Power Generation*, vol. 16, no. 13, pp. 2859–2880, 2022, doi: 10.1049/rpg2.12543.

BIOGRAPHIES OF AUTHORS



Raghad Adeeb Othman     obtained his Bachelor of Science in Electrical Engineering in 2002. In 2014, then obtained a Higher Diploma in Electrical Engineering/Power and Machine with a very good grade in "Study of Power Flow Using a Thyristor Controlled Series Capacitor (TCSC)". In 2023, then obtained my Master's degree with a very good grade in Electrical Engineering from the Department of Electrical Engineering, College of Engineering, University of Mosul, Iraq. The research title for the master's thesis is "Enhancement of Electrical Power System by Reactive Power Injection Via Hybrid System". She worked as an Assistant Engineer at the Ministry of Industry and Minerals/General Company for Food Products/Sugar and Yeast Factories in Mosul, Iraq, in 2003. She worked at Zarka.Net Internet and Communications Company in Mosul, Iraq, in 2004. After that, she was appointed as an Assistant Engineer at the University of Mosul/Computer Center in 2006. Then, she was appointed as an Assistant Chief Engineer in the Electrical Engineering Department, College of Engineering, University of Mosul. Now, she is an Assistant Lecturer in the Electrical Engineering Department, College of Engineering, University of Mosul. The areas of interest include renewable energy related to the smart grid and power systems. She can be contacted at email: raghadeeb@uomosul.edu.iq.



Omar Sharaf Al-Deen Yehya Al-Yozbaky     obtained his Bachelor of Science (B.Sc.) in Electrical Engineering in 2001 from the Electrical Engineering Department, College of Engineering, University of Mosul, Iraq. Then he was appointed as an assistant engineer in the same department. After that, he got an M.Sc. in "Overcome the effect of Critical distance in XLPE high voltage cables by inductive shunt compensator", 2008, from the same department as well. Upon his graduation, he was appointed as teaching staff (assistant lecturer) in the Electrical Engineering Department, College of Engineering, University of Mosul. In 2012, he obtained the scientific title (lecturer) and the Ph.D. degree in the Department of Electrical and Electronic Engineering, Faculty of Engineering, University Putra Malaysia in 2017. Since 2014, he has been a member of the Centre for Electromagnetic and Lightning Protection Research (CELP). Now, he is an Assistant Professor in the Electrical Engineering Department, College of Engineering, University of Mosul. The subjects of interest include renewable energy fields associated with the smart grid, thermal modeling, transformer design, and electrical machines. He can be contacted at email: o.yehya@uomosul.edu.iq.